

A Simple Passive Scalar Advection-Diffusion Model

Scott Wunsch

July 4, 2021

*The James Franck Institute, The University of Chicago
5640 South Ellis, Chicago, IL 60637, USA*

1 Abstract

This paper presents a simple, one-dimensional model of a randomly advected passive scalar. The model exhibits anomalous inertial range scaling for the structure functions constructed from scalar differences. The model provides a simple computational test for recent ideas regarding closure and scaling for randomly advected passive scalars. Results suggest that high order structure function scaling depends on the largest velocity eddy size, and hence scaling exponents may be geometry-dependent and non-universal.

PACSs: 47.27.GS; 05.40.+j

Keywords: Isotropic turbulence; Random processes; Passive scalars

2 Introduction

Passive scalars are ‘tracer particles’ which are advected by the flow of another fluid. A typical example might be ink mixed by flowing water. The mixing of a scalar field T in a velocity field \mathbf{u} is governed by the advection-diffusion equation,

$$(\partial_t + \mathbf{u}(\mathbf{x}, t) \cdot \nabla) T(\mathbf{x}, t) = D \nabla^2 T(\mathbf{x}, t) + f(\mathbf{x}, t) \quad (1)$$

in which D is a diffusion constant and f is an external source of scalar. The velocity field is determined independently of the scalar field (hence the adjective *passive*) and (in this discussion) is incompressible ($\nabla \cdot \mathbf{u} = 0$). The incompressible flow simply transports the scalar, without changing any of the scalar’s values. The diffusion term smooths the resulting scalar differences, while the source term generates new scalar to compensate for this smoothing.

The mixing of a scalar field T is characterized experimentally by its structure functions, defined as $S_{2n}(\mathbf{r}) \equiv \langle (T(\mathbf{x} + \mathbf{r}, t) - T(\mathbf{x}, t))^{2n} \rangle$ for positive integers n .

It has been established experimentally that passive scalar structure functions are scaling functions of r over a wide range of length scales when the advecting flow is turbulent. This range of length scales, known as the inertial range, extends from a macroscale (usually determined by the flow geometry) down to a dissipative cut-off scale. The lower end of the inertial scaling range is set either by the viscous scale of the velocity field (the scale where viscosity damps out the fluid motion) or by the scalar's dissipation scale (the scale where molecular diffusivity damps out scalar fluctuations). The ratio of these length scales, known as the Prandtl number, is a material property of the system. This work will focus exclusively on systems in which the molecular diffusivity imposes the lower bound on the inertial range (Prandtl number less than one). In such systems the size of the inertial range is measured by the Peclet number, defined as the ratio of the macroscale to the dissipation scale.

The inertial range scaling exponents ρ_{2n} , defined by $S_{2n}(r) \sim r^{\rho_{2n}}$, are measured experimentally. The simplest possible prediction is based on the belief that the scalar difference between two points separated by a distance r will typically have a magnitude $\Delta T(r)$ which scales with r , $\Delta T(r) \sim r^\beta$ (for some β). This implies $S_{2n}(r) \sim r^{2n\beta}$. Consequently, the scaling exponents satisfy $\rho_{2n} = n\rho_2$, which is known as ‘regular scaling.’ Experimentally, the exponents are seen to exhibit ‘anomalous scaling,’ $\rho_{2n} < n\rho_2$. Such scaling indicates that there is no typical magnitude for $\Delta T(r)$, and this wide variation in magnitudes is known as *multiscaling*. Experimentally, measured scaling indices for passive scalars in turbulent flows are quite anomalous. [1] Until recently, relatively little attention was paid to this observed anomalous scaling in the passive scalar field. This is perhaps because the phenomena had often been attributed to anomalous scaling of the underlying velocity field.

However, a model proposed by Robert Kraichnan [13] suggests that a hypothetical regular-scaling velocity field would still generate anomalous scaling in the scalar structure functions. In addition, the scaling exponents would be universal, independent of details such as the geometry of the flow. In this model, the passive scalar is advected by a stochastic velocity field with regular scaling in space but with an extremely short correlation time. It is possible to form equations for the structure functions in this model, provided a closure assumption is made. The proposed closure [13] [14] leads to structure functions which scale with r , but with scaling exponents ρ_{2n} which grow like \sqrt{n} rather than n . Others, however, have applied different techniques to the same model (avoiding a closure ansatz) and claim to have found different results. [8] [15] [2] [3] A review of the disagreement is given by Shraiman and Siggia. [16]

To study this closure ansatz and the passive scalar structure functions numerically, I use a one-dimensional model [10] in which the structure functions S_{2n} obey statistical equations with the same closure problem as in Kraichnan's model. The model is simple enough to allow direct numerical study of the structure function scaling (over 2 orders of magnitude in the separation r) and the proposed closure

ansatz. Mixing occurs through a random mapping function chosen to mimic an incompressible flow and induce scaling in the structure functions. Because it is restricted to one dimension, the model is best viewed as representing scalar mixing in a turbulent pipe flow.

In this model the second order structure function can be determined analytically. For large Peclet number it scales with r with a scaling exponent ρ_2 determined by the advective mapping function. The higher order structure functions $S_{2n}(r)$ also scale (numerically), with exponents ρ_{2n} which appear to approach a constant value at large n .

The closure ansatz proposed by Kraichnan is seen to fail in numerical simulations of this model. The source of this failure can be traced to the finite size of the largest mixing events. This upper length scale is analogous to the largest eddy size in a fluid flow (in a pipe this size is determined by the pipe diameter). Very large scalar differences cannot be produced by a single mixing event, but instead arise from the combined action of several events. For this reason large scalar differences are exponentially improbable. Deviations from the closure ansatz are observed only for these large scalar differences. However, the behavior of the large n structure functions is determined by these rare events. In this model the scaling exponents approach a constant at large n , in contrast to the \sqrt{n} behavior predicted for Kraichnan's model. In addition, the value of the constant might depend on the largest eddy size, so that the large n behavior of the exponents would be geometry dependent.

Because these conclusions rest primarily on the fact that the largest mixing events are much smaller than the system size, one might expect them to be independent of the details of the small-scale mixing process. Mixing in a turbulent pipe flow should exhibit this separation of length scales, and there is some experimental evidence to support the idea that large scalar differences are exponentially unlikely in such a flow. [9]

2.1 Kraichnan's Passive Scalar Model

Robert Kraichnan first introduced the 'white-advected' passive scalar model in 1968 [12], and introduced the anomalous-scaling solution in a pair of recent papers. [13] [14] All of the principal results of this section can be found in the recent literature, although some of the notation has been altered here.

In this model the passive scalar $T(\mathbf{x}, t)$ obeys the usual advection-diffusion equation,

$$(\partial_t + \mathbf{u}(\mathbf{x}, t) \cdot \nabla) T(\mathbf{x}, t) = D \nabla^2 T(\mathbf{x}, t) + f(\mathbf{x}, t) \quad (2)$$

in which D is a diffusion constant. The external source f was not explicitly considered by Kraichnan, but is necessary to maintain a state of statistical equilibrium. The incompressible velocity field ($\nabla \cdot \mathbf{u} = 0$) is random with zero mean and is white in time. The second order velocity structure function is specified as

$$\langle [\mathbf{u}(\mathbf{x} + \mathbf{r}, t) - \mathbf{u}(\mathbf{x}, t)] \cdot \frac{\mathbf{r}}{r} [\mathbf{u}(\mathbf{x} + \mathbf{r}, t') - \mathbf{u}(\mathbf{x}, t')] \cdot \frac{\mathbf{r}}{r} \rangle \equiv C \delta(t - t') \left(\frac{r}{L_v} \right)^\eta \quad (3)$$

where C is a constant and η is a parameter of the model. This scaling in space holds until r approaches some large correlation length L_v , representing the largest motions in the system. The scaling correlation in space is similar to real turbulent flows, while the very short range of temporal correlations is unphysical but desirable for technical reasons. The velocity statistics are chosen to be gaussian, so higher order velocity structure functions can be expressed in terms of this second order function. Consequently, the velocity structure functions exhibit regular scaling, and so any anomalous scaling found in the passive scalar structure functions must arise from the structure of the scalar advection-diffusion equation and not from the underlying velocity scaling.

The source term is also a gaussian random variable with zero mean. Its correlations are specified by

$$\langle f(\mathbf{x} + \mathbf{r}, t) f(\mathbf{x}, t') \rangle \equiv \chi(r) \delta(t - t'). \quad (4)$$

The spatial function $\chi(r)$ is assumed to be smooth, so that $\chi(r) \simeq \chi(0)$ for $r \ll L_s$, where L_s represents the correlation length of the source field.

Calculation of the structure functions proceeds by forming an equation for scalar differences at equal times, defined as $\Delta(\mathbf{x}, \mathbf{y}; t) \equiv T(\mathbf{x}, t) - T(\mathbf{y}, t)$. One can take the ensemble average of this equation by integrating over the recent history of the scalar and using the defined correlation functions for \mathbf{u} and f . The δ -correlation in time makes it possible to do the resulting integrals. Using the definition $S_{2n}(\mathbf{x} - \mathbf{y}) \equiv \langle \Delta^{2n}(\mathbf{x}, \mathbf{y}) \rangle$, the structure functions are found to obey

$$(\partial_t + \mathcal{L}) S_{2n} = J_{2n} + F_{2n}. \quad (5)$$

In this equation, \mathcal{L} is the Richardson eddy-diffusivity operator, defined as

$$\mathcal{L} S_{2n}(r) \equiv -2CL_v^{-\eta} r^{1-d} \partial_r (r^{\eta+d-1} \partial_r S_{2n}(r)) \quad (6)$$

where $r \equiv |\mathbf{x} - \mathbf{y}|$ and d is the dimension of space. The source term

$$F_{2n} \equiv 2n(2n - 1) S_{2n-2} (\chi(0) - \chi(r)) \quad (7)$$

was makes it possible to establish a state of statistical equilibrium ($\partial_t S_{2n} = 0$). The dissipation function

$$J_{2n} \equiv 2nD \langle \Delta^{2n-1} (\nabla_x^2 + \nabla_y^2) \Delta \rangle \quad (8)$$

must be expressed in terms of S_{2n} before the system of equations for S_{2n} will be closed.

The lowest non-trivial structure function, $n = 1$, can be determined exactly. The dissipation function J_2 can be evaluated by commuting derivatives with Δ and with the averaging process $\langle \dots \rangle$, so that

$$J_2 = 2D \nabla_r^2 S_2(r) - 4D \langle (\nabla T)^2 \rangle. \quad (9)$$

The mean-squared scalar dissipation $D\langle(\nabla T)^2\rangle$ is constant, and can be determined by balancing against the scalar source (since the flux of scalar is conserved). At very large separations $r \gg L_s$, the source correlation vanishes ($\chi(r) \rightarrow 0$) and S_2 must approach a constant. Consequently, the equation for S_2 implies $2D\langle(\nabla T)^2\rangle = \chi(0)$. The complete equation for S_2 can then be re-cast as

$$Cr^{1-d}\partial_r(r^{d-1}\left(\frac{r}{L_v}\right)^\eta\partial_r S_2(r)) + Dr^{1-d}\partial_r(r^{d-1}\partial_r S_2(r)) = \chi(0) \quad (10)$$

assuming $\chi(r) \simeq \chi(0)$. The two differential operators which act on S_2 possess different scalings. The length scale at which the operators are equal is defined as the dissipation scale, r_d :

$$r_d \equiv L_v \left(\frac{D}{C}\right)^{\frac{1}{\eta}}. \quad (11)$$

The upper limit of the inertial (scaling) range is set by the lesser of the two macroscales, L_s and L_v . In the inertial range ($r_d \ll r \ll \min(L_s, L_v)$), the second operator can be neglected, and the solution is approximately

$$S_2(r) \simeq \frac{\chi(0)L_v^2}{C\rho_2 d} \left(\frac{r}{L_v}\right)^{\rho_2} \quad (12)$$

where $\rho_2 \equiv 2 - \eta$ is the second-order scaling exponent. Alternately, in the dissipation range ($r \ll r_d$), the first operator can be neglected, and the solution is approximately

$$S_2(r) \simeq \frac{\chi(0)}{2Dd} r^2. \quad (13)$$

There are two possible approaches for determining the higher order scaling exponents. The first is to balance the eddy-diffusivity operator against the forcing term. If the $2n$ -th structure function has scaling exponent ρ_{2n} , then the corresponding eddy-diffusivity term scales with r with the scaling exponent $\rho_{2n} - \rho_2$. The source term has scaling ρ_{2n-2} . If these terms are equal (*i.e.* if J_{2n} is negligible) then the scaling exponents are given by $\rho_{2n} = n\rho_2$, which is regular scaling.

The other possibility, first proposed by Kraichnan [13], is to balance the eddy-diffusivity operator against the dissipation term J_{2n} . This basically assumes that the dominant scaling is set not by the source term, but by a homogeneous solution (or *zero mode*) of the structure function equations. Consequently, the scaling could be *universal*, independent of the details of the source term.

Unfortunately, evaluation of the J_{2n} requires a closure ansatz stating how the laplacian of the scalar field at two distinct points, $(\nabla_x^2 + \nabla_y^2)\Delta(\mathbf{x}, \mathbf{y})$ depends on the scalar difference $\Delta(\mathbf{x}, \mathbf{y})$ between those points. The proposed closure ansatz is best understood in terms of the probability distribution function (PDF) for scalar differences $P(\Delta, r)$. This function gives the probability for seeing a particular value Δ for the scalar difference between two points separated by a distance r . The structure functions $S_{2n}(r)$ are the moments of this PDF:

$$S_{2n}(r) \equiv \int P(\Delta, r)\Delta^{2n}d\Delta. \quad (14)$$

The unknown closure information is expressed in the conditional probability

$$H(\Delta, \mathbf{x} - \mathbf{y}) \equiv \langle (\nabla_x^2 + \nabla_y^2) \Delta(\mathbf{x}, \mathbf{y}) | \Delta(\mathbf{x}, \mathbf{y}) \rangle \quad (15)$$

which gives the ensemble-averaged value of $(\nabla_x^2 + \nabla_y^2) \Delta(\mathbf{x}, \mathbf{y})$ subject to the constraint that the scalar difference between the two points take on the particular value Δ . The dissipation functions can be expressed using H and the PDF for scalar differences $P(\Delta, r)$:

$$J_{2n}(r) = 2nD \int P(\Delta, r) \Delta^{2n-1} H(\Delta, r) d\Delta. \quad (16)$$

The closure ansatz proposed in [14] is that H is approximately a linear function of Δ :

$$H(\Delta, r) \cong \alpha(r) \Delta \quad (17)$$

with some unknown slope α . This assumption can be viewed as a truncation of the Taylor series expansion of $H(\Delta)$ (by symmetry, the series has only odd terms). By substitution, the dissipation functions are $J_{2n} = 2nD\alpha S_{2n}$. The function α can be determined by considering the $n = 1$ case. The result is that

$$J_{2n} = nJ_2 \frac{S_{2n}}{S_2} \quad (18)$$

(recall J_2 is approximately constant in the inertial range). Hence both J_{2n} and $\mathcal{L}S_{2n}$ have scaling exponent $\rho_{2n} - \rho_2$. Consequently, the scaling exponents are set by the *coefficients* of the terms. The result is that

$$\rho_{2n} = \frac{1}{2} \sqrt{4nd\rho_2 + (d - \rho_2)^2} - \frac{1}{2}(d - \rho_2). \quad (19)$$

The asymptotic behavior is that $\rho_{2n} \simeq \sqrt{nd\rho_2}$, which depends only on the spatial dimension d and the velocity scaling η (through $\rho_2 = 2 - \eta$).

2.2 Competing Calculations

The anomalous scaling for ρ_{2n} in the Kraichnan model depends on the closure ansatz, $H(\Delta) \propto \Delta$. Unfortunately, it is not possible to consider higher order corrections to the Taylor series for $H(\Delta)$ because the resulting equations for S_{2n} cannot be solved. However, others have approached the model using techniques which avoid the need for a closure ansatz and, in certain limits, have found values of ρ_{2n} which disagree with Kraichnan's result.

The competing approach to determining scaling exponents in this model focuses on the n -point correlation functions of the scalar (known as n th order moments), defined as

$$M_n(\mathbf{x}_1, \mathbf{x}_2, \dots, \mathbf{x}_n) \equiv \langle T(\mathbf{x}_1) T(\mathbf{x}_2) \dots T(\mathbf{x}_n) \rangle. \quad (20)$$

The n th order structure function can be expressed in terms of the corresponding moment by allowing points to fuse together. The moments convey more information than the structure functions and can be viewed as the more fundamental objects, but moments are generally not measured experimentally.

The δ -correlation in time makes it possible to construct closed equations for the moments (known as *Hopf* equations). There is no closure problem associated with the dissipative terms. Unfortunately, the equation of the n th order moment is a partial differential equation in $n!$ vector separations, and it is beyond the reach of known mathematics to determine the solutions of such complicated equations.

To determine scaling exponents, several groups have assumed an overall scaling for the n th order moment when all separations lie within the inertial range, and then attempted to calculate the scaling exponent in certain limits using perturbation theory. In each case it is assumed that the dominant contribution comes from a zero mode of the Hopf equation. These exponents differ from the structure function scaling exponents proposed by Kraichnan. The most readable description of this approach can be found in the paper by Chertkov, *et. al.* [2]

One of the first of these calculations was done in the limit $\rho_2 \rightarrow 2$. [8] The result was that the 4th order scaling exponent was given by

$$\rho_4 \simeq 2\rho_2 - \frac{4}{d+2}\eta \quad (21)$$

($\eta = 2 - \rho_2 \ll 1$). This indicates that the scaling is nearly regular in this limit, with a small correction for $\rho_2 < 2$. The solution proposed by Kraichnan (equation 19) is not regular in this limit; instead it yields

$$\rho_4 = \left(\frac{1}{2} \sqrt{d^2 + 12d + 4} + 1 - \frac{1}{2}d \right) - \frac{1}{2} \left(\frac{2 + 3d}{\sqrt{d^2 + 12d + 4}} - 1 \right) \eta \quad (22)$$

which is quite anomalous as $\eta \rightarrow 0$ (in three dimensions $\rho_4 \rightarrow 3$, not 4). This disagreement is very substantial. Unfortunately, the huge difference in approach makes it difficult to ascertain the source of the disagreement.

Another limit in which a discrepancy was found is the limit of large space dimension ($d \rightarrow \infty$). [2] [3] In this case the scaling is again nearly regular, with a small correction in $1/d$. The corresponding limit of equation 19 is also regular, but the correction term differs from that obtained from the Hopf equation calculation.

One proposed reconcilliation between these calculations is a generalization of Kraichnan's closure based on the 'fusion rules.' [5] The dissipation functions are given by a generalized form of equation 18

$$J_{2n} = nC_n J_2 \frac{S_{2n}}{S_2} \quad (23)$$

with an unknown constant of proportionality C_n . Values $C_n \neq 1$ would change the result for the scaling exponents to

$$\rho_{2n} = \frac{1}{2} \sqrt{4nC_n d \rho_2 + (d - \rho_2)^2} - \frac{1}{2}(d - \rho_2). \quad (24)$$

No precise form for C_n has been proposed, but Ching [6] argues that $C_n \propto n$ for large n , indicating $\rho_{2n} \propto n$ for large n .

Numerical simulations of the Kraichnan model in two dimensions have been attempted by two groups. [14] [7] Although the size of the inertial range is limited, both groups claim to support Kraichnan's solution for intermediate values of ρ_2 . The limit $\rho_2 \rightarrow 2$ has not been approached in either case.

3 A Simple One-Dimensional Model

3.1 Definition of the Model

To address the debate, I propose a simple passive scalar model which reproduces the closure problem described above. The closure ansatz can be studied numerically on two levels. First, one can calculate the dissipation functions J_{2n} and measure the constants of proportionality to determine if $C_n \neq 1$. Second, one can study the conditional probability $H(\Delta, r)$ directly to determine if it is a linear function of Δ .

For numerical simulations, it is necessary to develop a model which is simple enough computationally to permit a large inertial range. Consequently, a one-dimensional scalar field is preferable. However, a one-dimensional incompressible velocity field would be quite dull, so we are forced to choose some other form of mixing that retains certain traits of an incompressible flow. The attribute preserved in this model is that the mixing simply re-arranges the scalar field, without altering any scalar values. Any advection of this type will necessarily be non-local. The particular method of re-arrangement is based on a picture of a turbulent flow consisting of many swirling eddies, and is constructed to induce scaling in the passive scalar structure functions. Because the model is one-dimensional, it is best thought of as being analogous physically to a turbulent pipe flow. This model is loosely based on the 'linear eddy model' of Kerstein. [11]

The model is designed to produce structure functions which obey statistical equations with the same form as equation 5. The dissipation functions J_{2n} are identical, so that the closure problem is reproduced, but the eddy-diffusivity operator \mathcal{L} is altered (although it remains a scaling operator).

The motivation for this particular model is developed as follows: Imagine that the one-dimensional scalar field is embedded in a plane. The advection consists of an eddy in that plane, centered on the scalar field, which rotates one-half turn. This maps the scalar field $T(x)$ onto itself, according to the rule

$$T(x) \rightarrow T(L - x) \tag{25}$$

where L is the eddy size (centered on $x = \frac{1}{2}L$). The eddy acts only on the region $0 < x < L$; elsewhere nothing happens. Applying one of these eddies in each time step τ , with randomly chosen size and position, along with diffusion, gives a rule for advancing the state of the passive scalar by one time step,

$$T(x, \tau) = T(x, 0) + V[T(x, 0)] + D\tau\partial_x^2T(x, 0) \tag{26}$$

in which the advection operator $V[T]$ is

$$V[T(x)] \equiv \begin{cases} T(2x_o + L - x) - T(x) & \text{if } x_o \leq x \leq x_o + L, \\ 0 & \text{otherwise.} \end{cases} \quad (27)$$

The model consists of applying this rule many times, with the size L and position x_o chosen randomly at each step from appropriate probability distribution functions. All possible x_o in the system have equal probability, but the eddy sizes L are chosen according to a scaling probability with scaling index y :

$$P(L)dL = CL^{-y}dL. \quad (28)$$

This generates scaling behavior within an inertial range determined by the smallest and largest possible values of L : $L_o < L < L_v$. In the analogy to turbulent pipe flow, L_v would play the role of the pipe diameter and L_o the role of a viscous cut-off scale (the size of the smallest motions). The passive scalar structure functions would be expected to exhibit inertial range scaling between L_o and L_v , so long as the dissipation scale is not larger the L_o . In practice, the constant $D\tau$ is chosen so that the dissipation scale is roughly equal to L_o (corresponding to a Prandtl number near unity), so that the ratio of length scales $\frac{L_v}{L_o}$ plays the role of the Peclet number in the model.

To maintain a state of statistical equilibrium, some forcing is required. In this model, the forcing is done by imposing an overall gradient g on the scalar, as in [15]. A new variable θ is then defined by the deviation from the gradient,

$$\theta(x) \equiv T(x) - gx \quad (29)$$

and structure functions are defined in terms of θ :

$$S_n(r) \equiv \langle (\theta(x+r) - \theta(x))^n \rangle. \quad (30)$$

3.2 Structure Function Equations

Equations for the structure functions $S_n(r)$ can be constructed in the same way as in Section 1.2. The scalar difference $\Delta(x, y) \equiv \theta(x) - \theta(y)$ obeys the equation

$$\Delta(x, y; \tau) = D\tau(\partial_x^2 + \partial_y^2)\Delta(x, y; 0) + \Psi[\Delta(x, y; 0)] \quad (31)$$

when time is advanced by one unit τ . The action of the convective term Ψ on Δ depends on whether x or y (or both) lie within the eddy:

$$\Psi[\Delta(x, y)] \equiv \begin{cases} \Delta(x, y) & x, y \notin [x_o, x_o + L] \\ \Delta(2x_o + L - x, y) + g(L + 2x_o - 2x) & x \in [x_o, x_o + L], \\ & y \notin [x_o, x_o + L] \\ \Delta(x, 2x_o + L - y) - g(L + 2x_o - 2y) & x \notin [x_o, x_o + L], \\ & y \in [x_o, x_o + L] \\ \Delta(2x_o + L - x, 2x_o + L - y) - 2g(x - y) & x, y \in [x_o, x_o + L]. \end{cases} \quad (32)$$

Raising this equation to the n th power and taking the ensemble average gives

$$S_n(x-y; \tau) = \langle \Psi^n[\Delta(x, y; 0)] \rangle + nD\tau \langle \Psi^{n-1}[\Delta(x, y; 0)](\partial_x^2 + \partial_y^2)\Delta(x, y; 0) \rangle + \dots \quad (33)$$

keeping only the lowest order term in $D\tau$. In the diffusive term, $\Psi[\Delta]$ can be replaced with Δ , because only a small portion of the scalar field lies within the eddy at that time step (the eddy is another higher order correction). Then the equation becomes

$$S_n(x-y; \tau) = \langle \Psi^n[\Delta(x, y; 0)] \rangle + J_n(x, y; 0) \quad (34)$$

where

$$J_n(x, y) \equiv nD\tau \langle \Delta(x, y)^{n-1}(\partial_x^2 + \partial_y^2)\Delta(x, y) \rangle \quad (35)$$

as in equation 8 and [13]. The quantity $\langle \Psi^n[\Delta(x, y; 0)] \rangle$ can be computed from the definition of Ψ by taking the ensemble average over the eddy probabilities for x_o and L . Defining the difference variable $r \equiv x - y$, the result divides into three regions: a diffusive interval ($r \leq L_o$), the inertial range ($L_o \leq r \leq L_v$), and a large scale region ($r \geq L_v$). The structure functions obey the equation

$$\Lambda(S_n(r, \tau) - S_n(r, 0)) + \mathcal{L}[S_n(r, 0)] = \Lambda J_n(r, 0) + F_n(r, 0) \quad (36)$$

where Λ is the system size. In statistical equilibrium $S_n(r, \tau) = S_n(r, 0)$, and this equation is identical in form to equation 5. The eddy-diffusivity operator \mathcal{L} and the source $F_n(r)$ differ according to the value of r . For $r \leq L_o$, they are

$$\mathcal{L}[S(r)] \equiv - \int_{L_o}^{L_v} P(L)dL \left\{ \int_{L-r}^{L+r} dz S(z) - (r+L)S(r) - (r-L)S(-r) \right\} \quad (37)$$

$$F_n(r) \equiv \sum_{m=1}^n \frac{g^m n!}{m!(n-m)!} \int_{L_o}^{L_v} P(L)dL \left\{ \int_{L-r}^{L+r} dz S_{n-m}(z)(z-r)^m + (L-r)S_{n-m}(-r)(-2r)^m \right\}. \quad (38)$$

In the inertial range, $L_o \leq r \leq L_v$, they are

$$\begin{aligned} \mathcal{L}[S(r)] &\equiv - \int_{L_o}^r P(L)dL \left\{ \int_{r-L}^{r+L} dz S(z) - 2LS(r) \right\} \\ &- \int_r^{L_v} P(L)dL \left\{ \int_{L-r}^{L+r} dz S(z) - (r+L)S(r) - (r-L)S(-r) \right\} \end{aligned} \quad (39)$$

$$\begin{aligned} F_n(r) &\equiv \sum_{m=1}^n \frac{g^m n!}{m!(n-m)!} \left\{ \int_{L_o}^r P(L)dL \int_{r-L}^{r+L} dz S_{n-m}(z)(z-r)^m \right. \\ &\left. + \int_r^{L_v} P(L)dL \left\{ \int_{L-r}^{L+r} dz S_{n-m}(z)(z-r)^m + (L-r)S_{n-m}(-r)(-2r)^m \right\} \right\}. \end{aligned} \quad (40)$$

In the large scale region, $r \geq L_v$, they are

$$\mathcal{L}[S(r)] \equiv - \int_{L_o}^{L_v} P(L)dL \left\{ \int_{r-L}^{r+L} dz S(z) - 2LS(r) \right\} \quad (41)$$

$$F_n(r) \equiv \sum_{m=1}^n \frac{g^m n!}{m!(n-m)!} \int_{L_o}^{L_v} P(L)dL \left\{ \int_{r-L}^{r+L} dz S_{n-m}(z)(z-r)^m \right\}. \quad (42)$$

3.3 Solution for $S_2(r)$

The first order structure function S_1 vanishes, so the lowest non-trivial structure function is S_2 . It can be determined approximately in both the inertial and dissipative ranges. As a first step, it is necessary to re-write J_2 by commuting derivatives and using spatial homogeneity, as in the Kraichnan model:

$$J_2 = 2D\tau\langle\Delta(\partial_x^2 + \partial_y^2)\Delta\rangle = 2D\tau\partial_r^2 S_2 - 4D\tau\langle(\partial_x\theta)^2\rangle \quad (43)$$

where $D\tau\langle(\partial_x\theta)^2\rangle$ is the mean-square dissipation of the scalar (a constant). This constant can be evaluated by looking at the large scale region (where S_2 must approach a constant) and balancing it with the forcing term $F_2 = \frac{2}{3}g^2\langle L^3\rangle$, so that

$$\langle(\partial_x\theta)^2\rangle = \frac{1}{6}\frac{\langle L^3\rangle}{D\tau\Lambda}g^2. \quad (44)$$

This result serves as a check on the accuracy of numerical simulations.

The solution far into the dissipative region ($r \ll L_o$) can then be evaluated by neglecting both \mathcal{L} and F (setting $J_2 = 0$):

$$S_2(r) \cong \langle(\partial_x\theta)^2\rangle r^2 = \frac{1}{6}\frac{\langle L^3\rangle}{D\tau\Lambda}(gr)^2. \quad (45)$$

In the inertial range, the approximate solution is found by balancing the convective term \mathcal{L} against the dissipation term $J_2 \cong -4D\tau\langle(\partial_x\theta)^2\rangle$:

$$\mathcal{L}[S_2(r)] \cong -\frac{2}{3}\langle L^3\rangle g^2. \quad (46)$$

By assuming a scaling solution, $S_2(r) = A_2 r^{\rho_2}$, the convective term becomes

$$\mathcal{L}[A_2 r^{\rho_2}] \cong -\frac{A_2 L_o^y}{y-1} I(\rho_2, y) r^{2+\rho_2-y} \quad (47)$$

in the limits $\frac{L_o}{r} \rightarrow 0$ and $\frac{r}{L_v} \rightarrow 0$. The definite integral $I(\rho, y)$ is defined as

$$\begin{aligned} I(\rho, y) \equiv & \frac{1}{1+\rho} \left\{ \int_0^1 \frac{dz}{z^y} ((1+z)^{1+\rho} - (1-z)^{1+\rho} - 2(1+\rho)z) \right. \\ & \left. + \int_0^1 \frac{dz}{z^{3+\rho-y}} ((1+z)^{1+\rho} - (1-z)^{1+\rho} - 2(1+\rho)z^{1+\rho}) \right\} \end{aligned} \quad (48)$$

and can be evaluated numerically. The first integral in I diverges at the lower limit for $y > 3$, setting an upper limit on the scaling range. (For $y > 3$ the lower limit must be replaced by $\frac{L_o}{r}$, and the ultraviolet region determines the solution.) Since $\mathcal{L}[S(r)]$ balances a constant, the scaling is fixed at $\rho_2 = y - 2$ (which only makes sense for $y > 2$) and the solution for $L_o \ll r \ll L_v$ is

$$S_2(r) = \frac{2}{3} \frac{(gL_v)^2}{(2-\rho_2)I(\rho_2, y)} \left(\frac{r}{L_v}\right)^{\rho_2} \quad (49)$$

where $\langle L^3\rangle$ has been evaluated explicitly.

These solutions for S_2 compare very well with the numerical results in both the inertial and dissipative ranges (see Figure 2).

3.4 Higher Order Structure Functions

Even-Order Structure Functions

In the inertial range, the scaling of higher even-order structure functions is determined by balancing $\mathcal{L}[S_{2n}]$ against J_{2n} , as in [13]:

$$\mathcal{L}[S_{2n}(r)] \cong J_{2n}(r). \quad (50)$$

The closure assumption for J_{2n} is that

$$J_{2n}(r) = nC_n J_2 \frac{S_{2n}}{S_2}. \quad (51)$$

This generalized form with $C_n \neq 1$ was suggested in [5], while $C_n = 1$ gives the original Kraichnan ansatz of [13]. Assuming scaling functions for S_{2n} , the scaling exponents ρ_{2n} are determined by the coefficients in equation 50:

$$I(\rho_{2n}, y) = nC_n I(\rho_2, y) \quad (52)$$

This equation for the exponents is analogous to equation 24 in the Kraichnan model. This result can be used (in principle) to evaluate the coefficients of proportionality C_n given numerically measured ρ_{2n} . Unfortunately, the sensitivity of I to ρ limits the accuracy of this method. However, the numerical results for the exponents and C_n (computed from equation 51) are consistent with this result, indicating that the scaling is indeed set by balancing the convective term \mathcal{L} against the dissipation term J_{2n} .

Odd-Order Structure Functions

Odd order structure functions exhibit scaling only in the dissipative range. Because the eddy-diffusivity operator \mathcal{L} differs depending on whether it operates on an odd or even function of r , the inertial range scaling solution exists only for even order structure functions. Odd order functions are positive scaling functions in the dissipation range (small r), but pass through zero in the inertial range and then approach zero from below at large r . This behavior of the odd structure functions is peculiar to this particular model and differs from physical passive scalars.

3.5 Dissipation Range Scaling

At small enough length scales the dissipative terms determine the scaling. In this (dissipative) range the J_n term dominates the solution. It is convenient to re-write it as:

$$J_n(r) = 2D\tau\partial_r^2 S_n(r) - n(n-1)D\tau\langle\Delta^{n-2}[(\partial_x\theta)^2 + (\partial_y\theta)^2]\rangle. \quad (53)$$

Balancing the two parts of J_n against each other will lead to a solution if the conditional probability

$$G(\Delta, x-y) \equiv \langle[(\partial_x\theta)^2 + (\partial_y\theta)^2]|\Delta\rangle \quad (54)$$

can be calculated. In a purely dissipative system, G can be determined from a Taylor expansion of Δ at small separations: $\Delta \cong r(\partial_x \theta)$, which implies $G = \frac{2\Delta^2}{r^2}$. However, the presence of convection competes with the smoothing effects of diffusion and generates higher terms in the Taylor expansion of Δ . Given this fact, a reasonable closure approximation (which is supported numerically) is

$$G(\Delta, r) = a + \frac{b\Delta}{r} + \frac{c\Delta^2}{r^2} \quad (55)$$

where a , b , and c are constants. The assumed r dependence is necessary to generate a solution with regular scaling.

For a regular scaling solution, $S_n(r) = A_n r^n$, the unknown constants can be expressed in terms of A_2 (calculated above) and A_3 (unknown):

$$A_n = A_{n-2}A_2 + \frac{A_3}{A_2}A_{n-1}. \quad (56)$$

Hence all higher order structure functions are expressible in terms of S_2 and S_3 . Unfortunately, no analytic solution for S_3 has been found. However, in the absence of any spatial asymmetry (which is generated by the gradient forcing used in this model) the odd order structure functions would vanish and the solution would be

$$S_{2n}(r) = S_2^n(r) \quad (57)$$

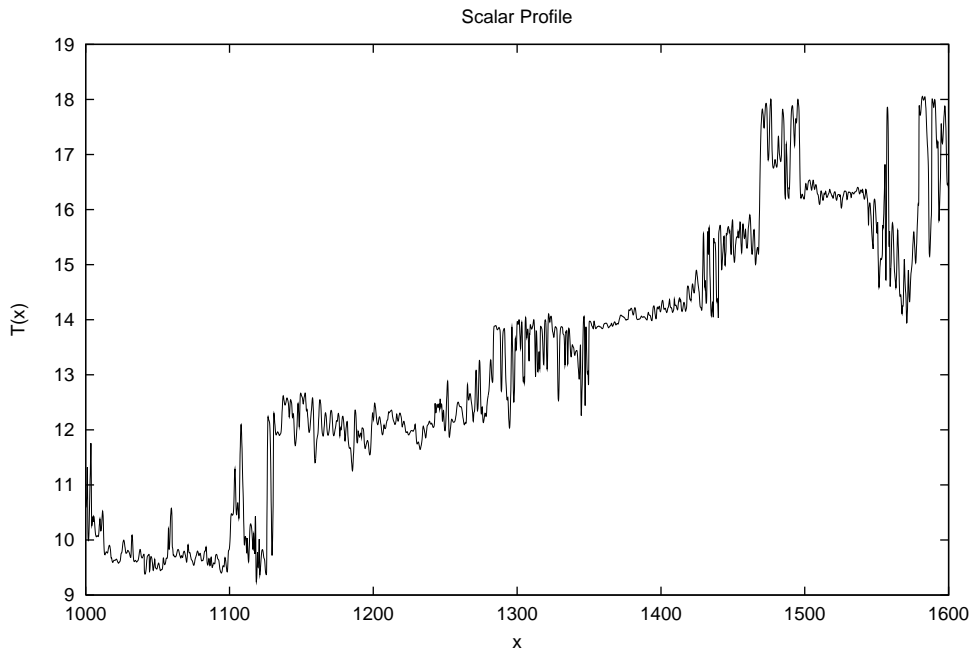
which has regular scaling but non-gaussian statistics.

4 Numerical Results

4.1 Simulation of the Model

A computational model was created by discretizing the dynamical equation for $T(x)$. The advective term is handled straightforwardly, since it is just a re-arrangement of the values of $T(x)$. Diffusion was done subsequent to the advection process in each time step, using a second-order implicit finite differences scheme. An overall gradient was applied to generate forcing, and periodic boundary conditions for the fluctuating field $\theta(x)$ were used. The system was evolved to a state of statistical equilibrium before any averaging computations were done. Equilibrium was indicated by the establishment of stable (analytically known) values of $\langle(\partial_x \theta)^2\rangle$ and $S_2(r)$. Structure functions were computed by taking space-time averages over the entire simulation, implicitly assuming an ergodic system.

Simulations were conducted in a system with 50000 grid points and a grid spacing of $dx = 0.1$. The smallest eddy size was $L_o = 2$, permitting a significant dissipative interval. The largest eddy size was either $L_v = 200$ or $L_v = 500$, allowing for inertial range scaling over two orders of magnitude. The imposed gradient was $g = 0.01$, and the diffusion constant $D\tau$ was of order 10^{-5} (varying slightly with y to set the



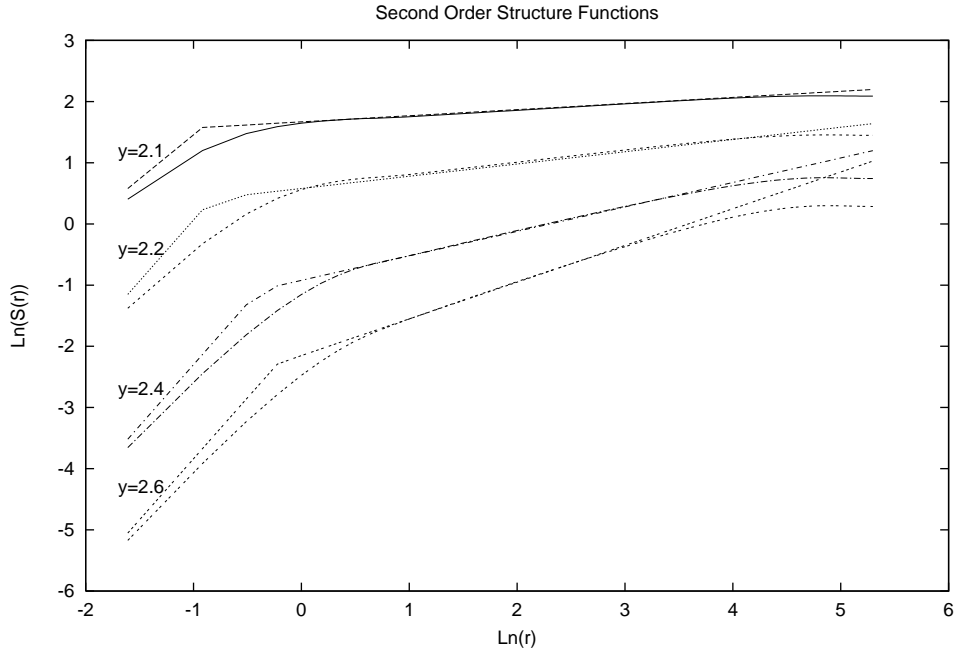
A ‘snapshot’ of the scalar profile, revealing the overall gradient $g = 0.01$ along with significant fluctuations. The profile represents 6000 grid points ($dx = 0.1$).

Figure 1: Typical Scalar Profile

dissipation scale approximately equal to L_o). The eddy scaling exponent was varied between $y = 2.1$ and $y = 2.8$ for $L_v = 200$, and between $y = 2.1$ and $y = 2.4$ for $L_v = 500$. The number of time steps varied between $3 \cdot 10^7$ and 10^8 . A large number of time steps is needed to suitably average over the eddy size probability distribution $P(L)$, especially for larger L_v and y . In addition, several simulations were conducted with large diffusion constants ($D\tau = 0.02$) to study the dissipative range solution. A typical ‘snapshot’ of the scalar profile $T(x)$ is shown in Figure 1. The profile reveals structure on a wide range of length scales, including significant ‘flat’ regions, and appears similar to experimentally observed profiles.

4.2 Numerically Computed Structure Functions

Second order structure functions S_2 have been computed analytically and can be compared directly with simulation results. Figure 2 shows S_2 as a function of r on a log-log plot (base e) for $L_v = 200$ and four values of y . The smooth curves show the simulation data (50 data points each). The analytic results are shown as two straight lines (equation 45 for the dissipative region, and equation 49 for the inertial range). There are no free parameters. The agreement is good (within 5% in the heart of the inertial range) except at the inertial range boundaries, where the analytic calculation has no validity. Interestingly, the boundary terms apparently

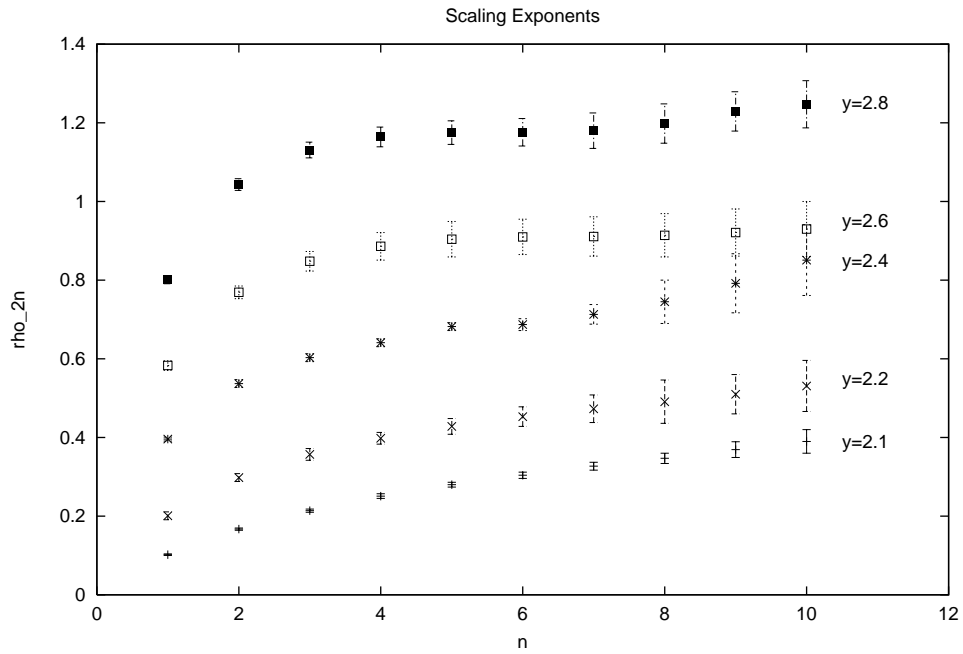


Second order structure functions $S_2(r)$ on a log-log plot, for $L_v = 200$ and four values of the scaling parameter y . Smooth curves are numerical simulation data; straight lines represent the analytic scaling solution in two regimes (inertial and dissipative ranges).

Figure 2: Second Order Structure Functions

grow in importance as y increases, and this encroachment reduces the effective size of the inertial range.

Higher even-order structure function also exhibit inertial range scaling. Figure 3 shows the even order scaling indices ρ_{2n} as a function of n for five values of y . The error bars represent the range of observed values over several simulations with different initial conditions. The scaling indices are independent of the upper length scale L_v (within the error). The second order indices ρ_2 lie within 3% of the theoretical values $y - 2$. The deviation from regular scaling ($\rho_{2n} = n\rho_2$) is quite pronounced. For larger y , the scaling exponents appear to approach a constant value (dependent on y) as n increases.

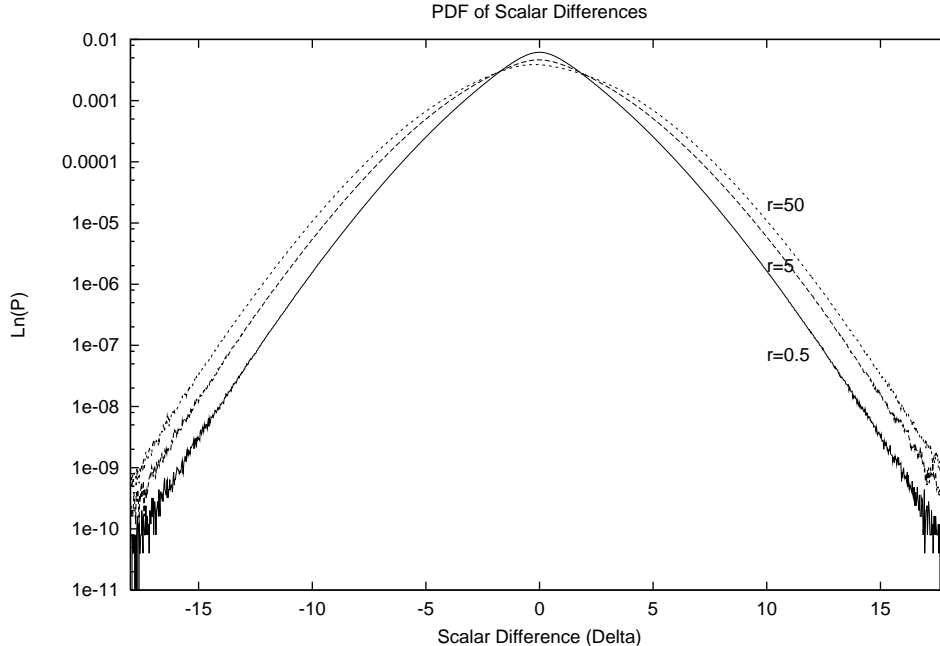


Inertial range structure function scaling exponents ρ_{2n} as a function of n for five values of y . These simulation data agree with the analytically known result $\rho_2 = y - 2$ for $n = 1$. The data suggest that the exponents may approach a constant value as $n \rightarrow \infty$.

Figure 3: Inertial Range Scaling Exponents

4.3 Probability Distribution Functions

Figure 4 shows the probability distribution function (PDF) for Δ on a log-linear scale for several values of r from the $y = 2.1$, $L_v = 200$ simulation. The core of the PDF, defined roughly by $|\Delta| \leq gL_v$ ($gL_v = 2$), is rounded. The slight asymmetry between positive and negative Δ is due to the imposed gradient. Figure 5 shows the PDFs for the same values of r from the $y = 2.4$, $L_v = 200$ simulation. The core of this PDF is much more sharply peaked.



Probability distribution function $P(\Delta)$ of scalar differences Δ for three separations r , from the $y = 2.1$, $gL_v = 2$ simulation. The tails ($|\Delta| > gL_v$) of the distribution appear to be exponential, with a slope which is independent of r .

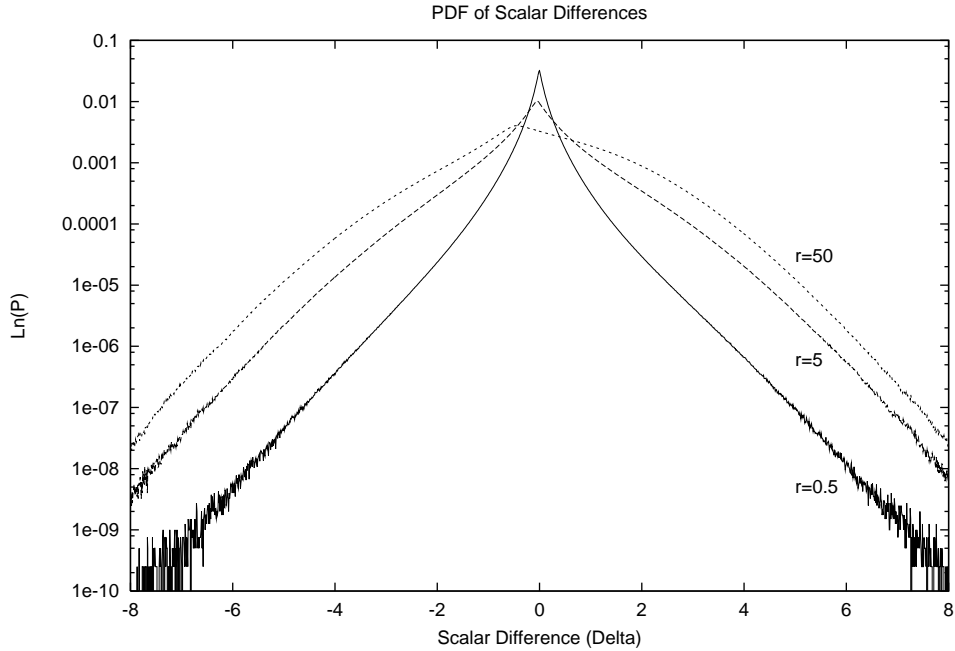
Figure 4: Scalar Difference PDF, $y = 2.1$

All the numerically generated PDFs exhibit exponential tails for $|\Delta| \gg gL_v$:

$$P(\Delta, r) \cong A(r)e^{-c|\Delta|} \quad (58)$$

where c is independent of the separation r . Exponential tails have also been derived in another model in a particular limit. [4] This form of the PDF suggests that, for large n , the structure function scaling exponents ρ_{2n} approach a constant independent of n . In this case the structure functions obey

$$\lim_{n \rightarrow \infty} \frac{S_{2n}}{S_{2n-2}} = \frac{2n(2n-1)}{c^2} \quad (59)$$



Probability distribution function $P(\Delta)$ of scalar differences Δ for three separations r , from the $y = 2.4$, $gL_v = 2$ simulation. The tails ($|\Delta| > gL_v$) of the distribution appear to be exponential, with a slope which is independent of r .

Figure 5: Scalar Difference PDF, $y = 2.4$

in the limit of large n . The PDF's and the structure functions can both be used to independently estimate c , and the results are shown in Figure 3.9 (as a function of ρ_2). The two sets of data represent the two different values of L_v , $L_v = 200$ and $L_v = 500$.

The exponential tails can be understood in terms of a random walk of fluid elements. To generate a particular temperature difference Δ , fluid elements initially separated by a distance of order $\frac{\Delta}{g}$ must be brought close together. Since the largest correlated motion in the system is of size L_v , scalar differences larger in magnitude than gL_v can only be generated by the uncorrelated action of several eddies. This behavior is essentially a random walk, and the multiplication of probabilities leads to the exponential PDF.

To be more quantitative, consider the probability for the motion of a fluid element along a Lagrangian trajectory from position zero to position x . For simplicity assume that all eddies are the same size L . To move a distance x with $(m-1)L \leq x \leq mL$ (for integer m) will typically require the point to be moved by m eddies, each carrying it a distance of order L . However, the probability that the point will lie within a

particular eddy is $\frac{L}{\Lambda}$, and these probabilities multiply:

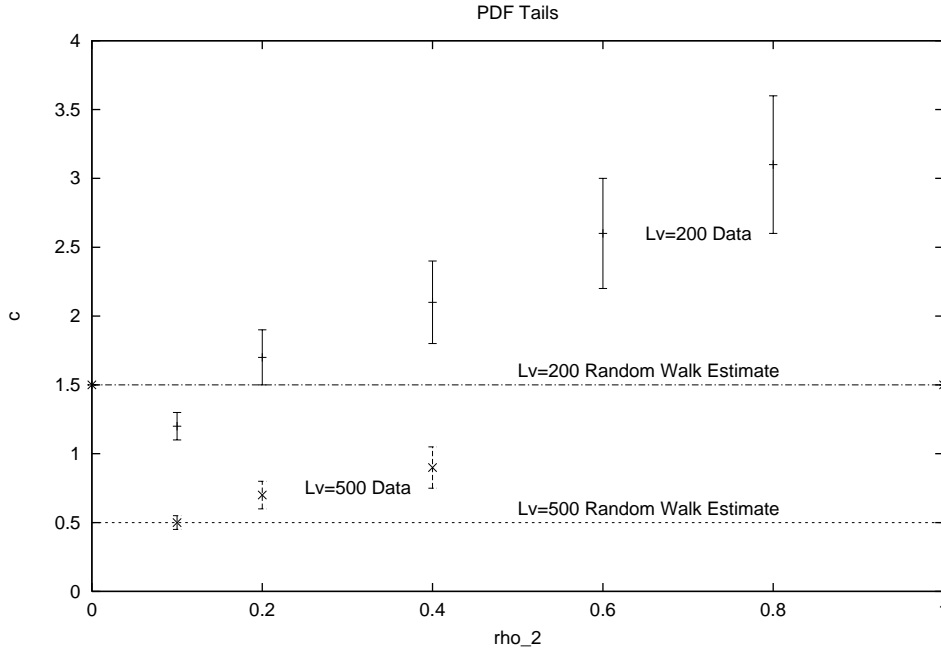
$$P(x \sim mL) \sim \left(\frac{L}{\Lambda}\right)^m. \quad (60)$$

The motion must occur quickly, in (order of magnitude) m steps, or else diffusion will cause the fluid element to equilibrate with its new environment. By assuming the two points involved in constructing Δ move independently, this probability can be converted to a PDF for Δ by using $x \sim \frac{\Delta}{g}$ regardless of the separation r . The result is

$$P(\Delta) \sim e^{-c\Delta} \quad (61)$$

$$c \equiv \frac{1}{gL} \ln\left(\frac{\Lambda}{L}\right). \quad (62)$$

Assuming that each eddy is of size L_v suggests estimates of $c = 1.5$ for $L_v = 200$ and $c = 0.5$ for $L_v = 500$. These values are shown as straight lines in Figure 6, and are in qualitative agreement with the data. Of course, not all eddies are of size L_v ; in fact the number of large eddies decreases as ρ_2 increases. This results in the trend of increasing c shown in Figure 6.



Slopes c of the tails of the PDF $P(\Delta)$ measured from simulation data for $L_m = 200$ and $L_m = 500$. The straight lines represent the Lagrangian random-walk estimate of c . The dependence on ρ_2 arises because large eddies become less frequent as ρ_2 increases.

Figure 6: Slopes of PDF Tails

Once two particles have come close together, they become subject to correlated motions and diffusion. This is presumably the source of the r dependence in the prefactor $A(r)$ of the exponential tail. Correlated motions have a weak influence on the PDF tail, and cannot alter its exponential character. Also, there is a slight asymmetry between Δ and $-\Delta$ in the prefactor; this is attributed to the fact that producing a negative Δ requires the two points to pass by each other (in one dimension), and during this time their motion is correlated.

4.4 Kraichnan's Closure Ansatz

To test the closure ansatz in [13] and evaluate the constants of proportionality C_n , the dissipation functions J_{2n} were computed directly from the simulation data. Rather than use the Laplacian, J_{2n} was re-written by commuting derivatives as

$$J_{2n}(r) = 2D\tau\partial_r^2 S_{2n}(r) - 2n(2n-1)D\tau\langle\Delta^{2n-2}[(\partial_x\theta)^2 + (\partial_y\theta)^2]\rangle. \quad (63)$$

In the limit $D\tau \rightarrow 0$, only the second term on the right side remains. In actual simulations, the first term makes a finite contribution which makes it more difficult to determine the inertial range scaling. So in practice only the second term (approximated using finite differences) was used as a surrogate for J_{2n} in the inertial range.

In the inertial range, the J_{2n} are scaling functions of r with scaling indices q_{2n} which, by the closure ansatz, ought to satisfy

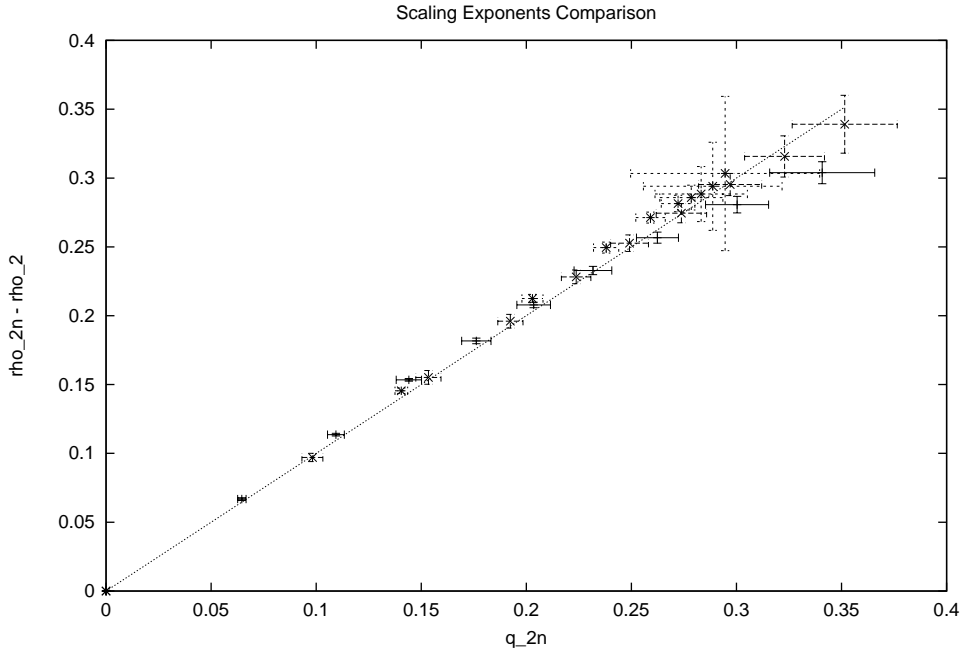
$$q_{2n} = \rho_{2n} - \rho_2. \quad (64)$$

Figure 7 shows that this part of the closure ansatz holds, by plotting q_{2n} vs. $\rho_{2n} - \rho_2$ for the $L_v = 500$ simulations.

The constants C_n can be computed using $C_n = \frac{J_{2n}S_2}{nJ_2S_{2n}}$ and averaging over the inertial range (C_n is approximately constant over the region averaged). The resulting values do not appear to depend on any parameters of the system other than y (a weak dependence on L_v is suspected but not detectable). Figure 8 shows computed values for C_n averaged over several simulations. The deviation from $C_n = 1$ is small but significant, contradicting the ansatz of [13]. The growing values of C_n at small ρ_2 suggests near-regular scaling in this limit, at least for moderate values of n . This is consistent with the scaling exponents in Figure 3. The intermediate case $\rho_2 = 0.4$ lies very close to the Kraichnan prediction of $C_n = 1$. For larger ρ_2 , C_n decreases with n , consistent with the scaling exponents approaching a constant value (as in Figure 3).

In [14], the closure ansatz in [13] is derived from an assumption about a conditional probability, namely that

$$H(\Delta, x-y) \equiv \langle(\partial_x^2 + \partial_y^2)\Delta(x,y)|\Delta(x,y)\rangle = \left(\frac{J_2}{2D\tau S_2}\right)\Delta. \quad (65)$$



Inertial range scaling exponents q_{2n} for the dissipation functions J_{2n} compared to the structure function scaling exponents ρ_{2n} . Kraichnan's closure ansatz requires $q_{2n} = \rho_{2n} - \rho_2$, and the simulation data is consistent with this result.

Figure 7: Scaling Exponent Comparison

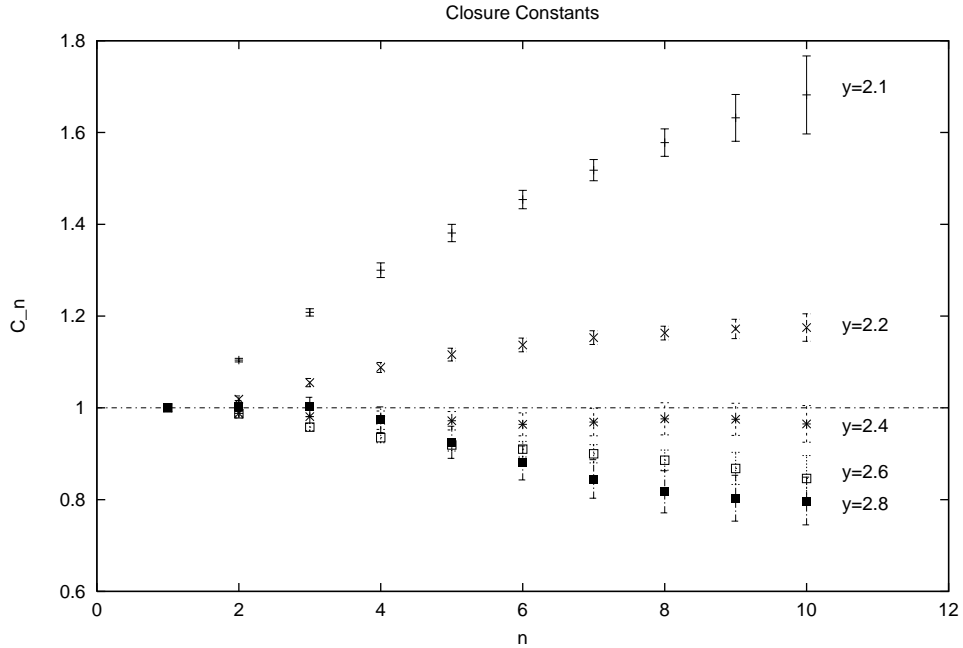
This conditional probability $H(\Delta, r)$ has been computed numerically in the simulations. Figure 9 shows $H(\Delta)$ as a function of Δ , normalized by $\frac{J_2}{2D\tau S_2}$, for $\rho_2 = 0.1$ and both $L_v = 200$ and $L_v = 500$. Two values of r are shown for each simulation. The resulting averages lie very close to $H(\Delta) = \Delta$ for small Δ , as assumed in [14]. However, they deviate from the straight line at $|\Delta| \cong 2gL_v$. This is approximately the point at which correlated motion becomes unimportant and the dynamics are controlled by the 'random walk' described on the previous section. The failure of Kraichnan's ansatz appears to be due to the existence of a finite upper size of the inertial range, L_v , which is much smaller than the system size. Other values of ρ_2 exhibit a similar behavior.

Upon closer examination, the large n behavior of the constants of proportionality C_n can be related to the failure of the closure ansatz. Using the definition of the constants,

$$C_n \equiv \frac{J_{2n} S_2}{n J_2 S_{2n}} \quad (66)$$

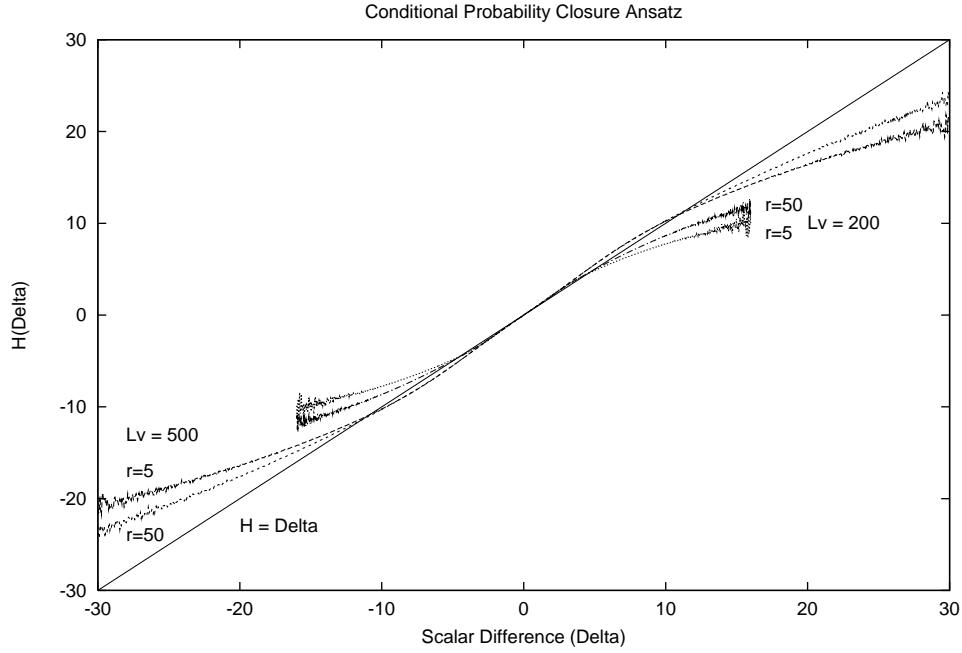
the C_n can be related to the closure ansatz through the definitions of S_{2n} and J_{2n} . These definitions are

$$S_{2n} \equiv \int P(\Delta) \Delta^{2n} d\Delta \quad (67)$$



Closure constants of proportionality C_n , defined by $J_{2n} = nC_n J_2 \frac{S_{2n}}{S_2}$, from simulation data for several y . Kraichnan's closure ansatz requires $C_n = 1$, which is inconsistent with the data. For larger y , C_n decreases with n , suggesting scaling exponents might approach a constant value at large n . For smaller y , C_n increases with n , suggesting near-regular scaling for moderate values of n . Both trends are consistent with the scaling exponents shown in Figure 3.

Figure 8: Closure Constants of Proportionality



Conditional probability $H(\Delta, x - y) \equiv \langle (\partial_x^2 + \partial_y^2) \Delta(x, y) | \Delta(x, y) \rangle$ as a function of the temperature difference Δ for two values of L_v and two separations $r = x - y$. Data from the $y = 2.1$ simulations. H is normalized so that $H = \Delta$ is the Kraichnan ansatz. The ansatz is in good agreement with the data for small values of Δ , but the data deviates for $|\Delta| > 2gL_v$ ($g = 0.01$). This is approximately the largest value of Δ which can be generated by a single large eddy; larger values are exponentially unlikely (see Figure 4).

Figure 9: Conditional Probability Closure Ansatz

and

$$J_{2n} \equiv nD\tau \int P(\Delta)\Delta^{2n-1}H(\Delta)d\Delta \quad (68)$$

where $P(\Delta)$ is the probability distribution function for scalar differences.

If one defines the ‘error’ in Kraichnan’s closure as δH

$$\delta H(\Delta) \equiv \Delta - \frac{2D\tau S_2}{J_2}H(\Delta) \quad (69)$$

then the closure constants can be written as

$$C_n = \frac{1 - Q_{2n}}{1 - Q_2} \quad (70)$$

where the functions Q_{2n} are defined as

$$Q_{2n} \equiv \frac{\int P(\Delta)\Delta^{2n-1}\delta H d\Delta}{\int P(\Delta)\Delta^{2n}d\Delta} \quad (71)$$

representing the contribution of the ‘error’ δH to C_n .

Numerically, δH is approximately zero for small $|\Delta|$, but appears to grow linearly with Δ for $|\Delta| > 2gL_v$. Asymptotically, $H(\Delta)$ might grow as fast as linearly with Δ (but with a slope less than one). An approximate large $|\Delta|$ form for H consistent with the simulation results is

$$H(\Delta) \simeq \alpha \frac{J_2}{2D\tau S_2} \Delta \quad (72)$$

where $0 \leq \alpha < 1$. Then $\delta H \propto (1 - \alpha)\Delta$ for $|\Delta| > 2gL_v$. Assuming this form for δH , the function Q_2 should be less than one. However, as $n \rightarrow \infty$, $Q_{2n} \rightarrow 1 - \alpha$. If the numerically observed trend for $H(\Delta)$ persists as $|\Delta| \rightarrow \infty$, this implies

$$\lim_{n \rightarrow \infty} C_n = \frac{\alpha}{1 - Q_2} \quad (73)$$

which is a constant. It would be consistent with the numerics to have $\alpha = 0$ and hence

$$\lim_{n \rightarrow \infty} C_n = 0. \quad (74)$$

It is also possible that α is non-zero and that $\frac{\alpha}{1 - Q_2}$ depends on ρ_2 . This might explain the possibly different asymptotic values for C_n for different values of ρ_2 seen in Figure 8.

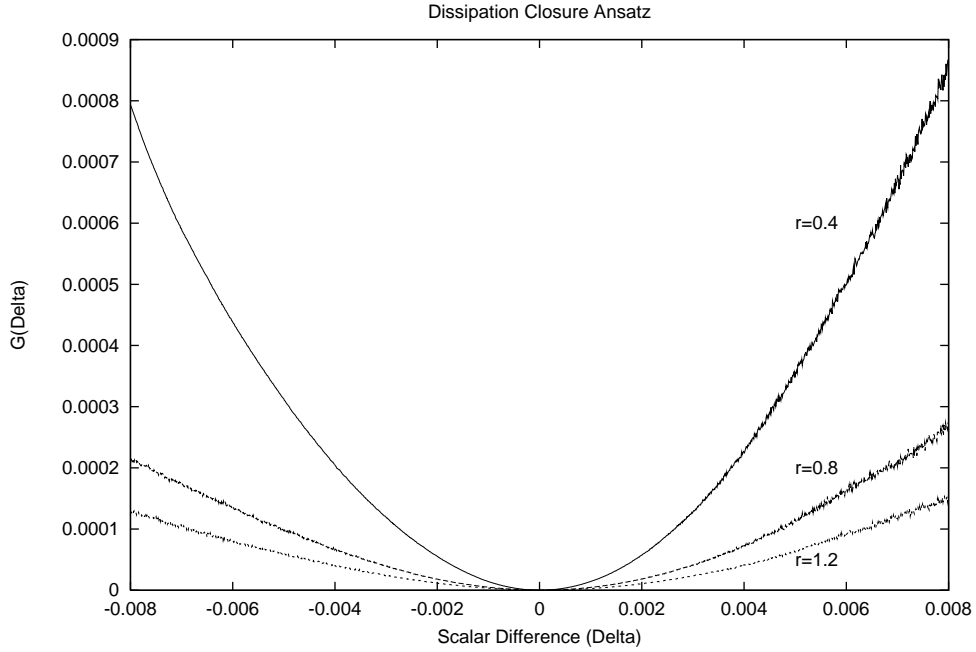
Unfortunately, in the Kraichnan model the truly interesting quantity is nC_n . For $\alpha = 0$, there are two possible asymptotic behaviors. If nC_n is bounded at very large n , the scaling exponents ρ_{2n} would approach a constant as $n \rightarrow \infty$ (as suggested for the eddy model). If instead nC_n is unbounded (but growing no faster than n), then ρ_{2n} would also be unbounded, but growing no faster than \sqrt{n} . The possibility that $nC_n \rightarrow 0$ is excluded by the Holder inequalities, since it would imply ρ_{2n} decreasing with n . If instead $\alpha > 0$, nC_n must grow linearly with n and the scaling exponents ultimately grow like \sqrt{n} , although the precise values may differ from the $C_n = 1$ prediction.

4.5 Dissipative Range Closure Ansatz

The conditional probability $G(\Delta)$ needed for closure in the dissipative range is shown in Figure 10 for several values of r (from the simulation with $D\tau = 0.02$). The conditional probabilities are well approximated by the parabola

$$G(\Delta, r) = a + \frac{b\Delta}{r} + \frac{c\Delta^2}{r^2} \quad (75)$$

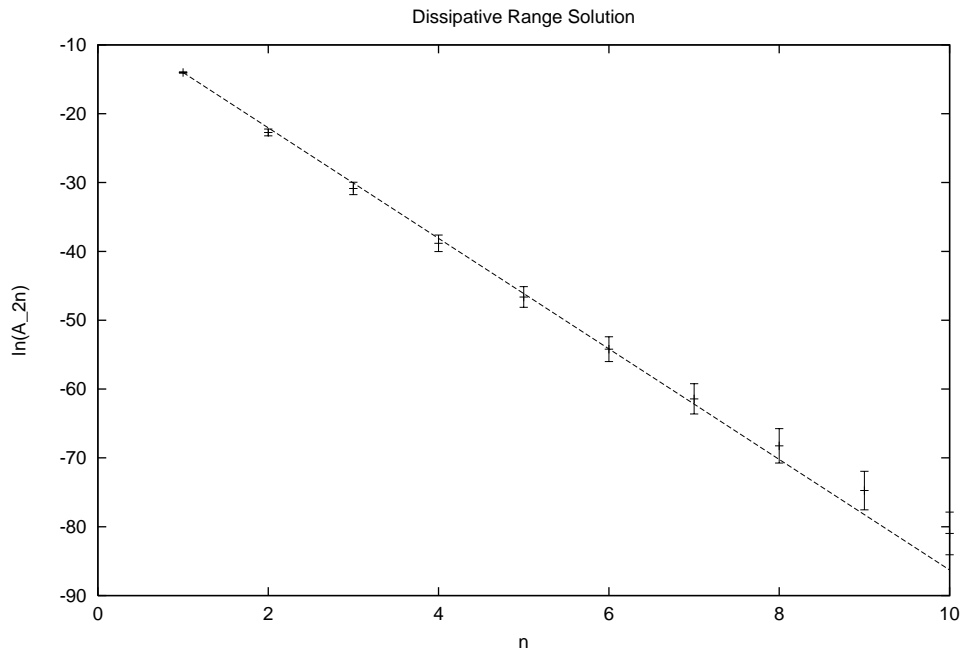
with $a \cong 4 \cdot 10^{-7}$, $b \cong 2 \cdot 10^{-3}$, and $c \cong 1.99$. These values are consistent with the independently known values of A_2 and A_3 .



Conditional probability $G(\Delta, x - y) \equiv \langle [(\partial_x \theta)^2 + (\partial_y \theta)^2] | \Delta(x, y) \rangle$ as a function of the temperature difference Δ for several values of $r \equiv x - y$ in the dissipative subrange. Data from the diffusion-dominated simulation. The parabolic form is consistent with the small-scale closure ansatz proposed in the previous chapter.

Figure 10: Dissipation Range Closure Ansatz

The structure functions are given by $S_n(r) = A_n r^n$, and the constants A_n are shown in Figure 11. In addition, the calculated values $A_n = A_{n-2} A_2 + \frac{A_3}{A_2} A_{n-1}$ from equation 56 are also shown, using the analytically known value of A_2 and the value of A_3 determined from fitting $S_3(r)$. The deviations from the analytic solution at large n are possibly due to the neglected terms F_n and \mathcal{L} in the equation for the structure functions.



Structure function coefficients A_{2n} as a function of n for the dissipative range regular-scaling solution, $S_{2n} = A_{2n}r^{2n}$. The data points were determined by fitting the simulation data. The straight line is the analytic solution, with the unknown parameter $\frac{A_3}{A_2}$ determined by fitting the numerical data for $S_3(r)$.

Figure 11: Dissipation Range Solution

5 Conclusions

5.1 Extensions to the Kraichnan Model

The original motivation for studying this ‘eddy model’ was to test the validity of the closure ansatz proposed in [14]. In the model, the principal failure of the closure could be traced to the finite size of the largest eddy, L_v . Specifically, the conditional probability $H(\Delta)$ is not a linear function of Δ , deviating at large values ($|\Delta| \gg gL_v$, where g is the imposed gradient). The deviation arises because the largest velocity eddy in the system (L_v) is much smaller than the system size, so that large scalar differences only occur as a result of the uncorrelated action of several eddies.

This finite L_v effect causes the constants of proportionality C_n proposed in [5] to deviate from 1, growing with n for small ρ_2 but shrinking with n at large ρ_2 (in contradiction to the predictions of [6] and also the simulations of [7]). Other apparent consequences of this effect include exponential tails for scalar difference PDFs and scaling exponents ρ_{2n} which approach a constant value at large n . Because this effect depends only on the existence of a finite eddy size L_v and not on the details of the smaller scale mixing, it is reasonable to expect that it might apply generically to other models of scalar mixing, including the one proposed by Kraichnan.

The limit $L_v \rightarrow \infty$

For small values of the scalar difference Δ ($|\Delta| < gL_v$) the numerical simulations of the eddy model appear to support the conditional probability ansatz $H(\Delta) \propto \Delta$. Low order structure functions should therefore have exponents ρ_{2n} which lie very close to the values predicted by Kraichnan. The fact that the errors become significant at large $|\Delta|$ means that the scaling exponents ρ_{2n} will exhibit deviations from the values predicted by this ansatz when one looks at sufficiently high order structure functions (large n).

Mathematically, structure function scaling is defined for an infinite inertial range, or $L_v \rightarrow \infty$. When considering the large n behavior of the scaling indices, one must take the limits $L_v \rightarrow \infty$ and $n \rightarrow \infty$. The order matters. If one considers small enough values of n (for any particular L_v) it will appear that Kraichnan is correct. Hence if one lets $L_v \rightarrow \infty$ first, all values of n will satisfy his predictions. For moderate values of ρ_2 the numerical simulations of the ‘eddy model’ support Kraichnan’s ansatz if the limits are taken in this order. However, for any finite L_v one can find sufficiently large n for which the scaling exponents deviate from the Kraichnan values due to the finite L_v effect. Hence if one lets $n \rightarrow \infty$ first, the Kraichnan solution will fail. It is my personal opinion that keeping L_v finite while letting $n \rightarrow \infty$ is the more physical limit, since any real system will have a finite largest eddy size.

The limit $\rho_2 \rightarrow 0$

There is some numerical evidence that regular scaling is approached in the limit $\rho_2 \rightarrow 0$ in the eddy model. The constants of proportionality deviate significantly from $C_n = 1$ even for the lowest values of n , and the lowest scaling exponents fall just below the regular scaling line $\rho_{2n} = n\rho_2$. In addition, the core of the scalar difference PDF becomes very rounded, perhaps gaussian, in this limit. The source of these effects is not understood, but it is very possible that they have nothing to do with the finite L_v effect. If so, they may indicate a failure of the Kraichnan ansatz which would persist in the limit $L_v \rightarrow \infty$. However, it must be remembered that direct calculation of the conditional probability $H(\Delta)$ does not indicate any measurable discrepancy with the closure ansatz for small values of Δ in this limit.

Comparison with other Calculations

In most of the competing calculations for the exponents of the Kraichnan model [2] [3] [8], the gradient forcing is replaced by a random source term for the passive scalar. In this formulation there are two upper length scales in the problem. They are the largest correlation length of the velocity field, L_v , and the largest correlation length of the source field, L_s . Whether or not one would expect to see deviations from Kraichnan's ansatz of the type observed in the eddy model depends on which of these two length scales is larger.

First, consider $L_s \gg L_v$. The source of the scalar is smooth over length scales much larger than the largest motions of the velocity field. In this case very large scalar differences can only be generated by uncorrelated transport over scales much larger than L_v . This is analagous to the transport against the gradient by random events in the eddy model. Hence in this case one might expect to see scalar difference PDFs with exponential tails, and deviations from Kraichnan's ansatz like those seen in the eddy model.

The opposite case is $L_s \ll L_v$. Then the largest 'globs' of scalar (of size L_s) can be mixed by coherent motions of the velocity field. The sort of transport described above would not happen, and the Kraichnan ansatz could be correct in this case. However, this is the order of limits taken in [2] [3] [8], and these authors claim to find deviations from the Kraichnan result. If they are correct, the deviations come from a different source than the finite L_v effect, so the eddy model simulations don't necessarily support their claims.

A recent paper by Chertkov, *et. al.*, [4], has more in common with the eddy model. It considers a scalar advected by a one-dimensional compressible velocity field with correlations analogous to the Kraichnan model. By assuming that the tails of the scalar difference PDF are dominated by the most rapidly stretched Lagrangian trajectories, they conclude that the tails must be exponential and that the scaling exponents ρ_{2n} must be independent of n . The calculations were done in the limit $\rho_2 \rightarrow 0$. Although the level of mathematical sophistication is quite different, the basic assumption is identical to the one used to understand the PDF tails in the

eddy model, and the conclusions are also similar.

5.2 Extensions to Pipe Flow

As suggested earlier, one can draw physical analogies between the eddy model and scalar mixing in turbulent pipe flow. In particular, the separation of length scales (between the largest eddy size and the system size) required for exponential tails in the scalar difference PDF can be achieved in pipe flow. The finite diameter of the pipe limits velocity eddies to this size, while the pipe itself can be much longer (analogous to this one-dimensional model). The mixing in the eddy model at small scales is quite different from real flows, but the likelihood of transport across distances larger than L_v (analogous to the pipe diameter) could be similar (statistically) to real pipes. This suggests that, for large n , the scaling exponents in pipe flows would approach a constant value. Further, since the slope of the PDF tails depends on the pipe diameter (gL_v), this value might be geometry-dependent.

Recent experiments on pipe flows [9] have revealed PDF's of scalar values with exponential tails. No attempt has been made to study scalar differences, but the arguments of the previous chapter suggest that exponential tails in the scalar value PDF would imply exponential tails in the scalar difference PDF. If true, this would force structure function scaling exponents in turbulent pipe flow to approach a constant (non-universal) value at large n .

Flows in other geometries (such as a box, for example), would not be expected to display this effect. If the largest velocity eddy is comparable to the system size, large-scale mixing can occur under the correlated motion of a single large eddy, and the mechanism for generating exponential tails in the PDF would not exist. Hence there is no reason to expect that scaling exponents ρ_{2n} would approach a constant at large n in such geometries. The structure function scaling exponents of the passive scalar might therefore be geometry-dependent, with pipes exhibiting a different large n asymptotic behavior than more open flow geometries.

6 Acknowledgements

It is a pleasure to acknowledge usefull discussions with L.P. Kadanoff, G. Falkovich, D. Lohse, P. Constantin, M. Chertkov, T. Zhou, and N. Schoegerhofer. This work was supported in part by a Fannie and John Hertz Foundation Fellowship. It also utilized MRSEC shared facilities under NSF-DMR grant number 9400379.

References

- [1] R. A. Antonia, E. J. Hopfinger, Y. Gagne, and F. Anselmet, Phys. Rev. A **30**, 2704 (1984).

- [2] M. Chertkov, G. Falkovich, I. Kolokolov, and V. Lebedev, *Phys. Rev. E* **52**, 4924 (1995).
- [3] M. Chertkov, G. Falkovich, and V. Lebedev, *Phys. Rev. Lett.*, **76**, 3707 (1996).
- [4] M. Chertkov, I. Kolokolov, and M. Vergassola, “Inverse cascade and intermittency of passive scalar in 1d smooth flow,” preprint (1997).
- [5] E. Ching, V. S. L’vov, and I. Procaccia, *Phys. Rev. E* **54**, 4520 (1996).
- [6] E. Ching, ”Scaling Constraints for a White-Advection Passive Scalar,” preprint (1997).
- [7] A. Fairhall, B. Galanti, V. L’vov, I. Procaccia, “Direct numerical simulations of the Kraichnan model,” preprint (1997).
- [8] K. Gawedzki and A. Kupianen, *Phys. Rev. Lett.* **75**, 3834 (1995).
- [9] J. E. Guilkey, A. R. Kerstein, P. A. McMurtry, and J. C. Klewicki, *Phys. Rev. E* **56**, 1753 (1997).
- [10] L. P. Kadanoff, S. Wunsch, T. Zhou, *Physica A* **244**, 190 (1997).
- [11] A. R. Kerstein, *J. Fluid Mech.* **231**, 261 (1991).
- [12] R. Kraichnan, *Phys. Fluids* **11**, **64**, 945 (1968).
- [13] R. Kraichnan, *Phys. Rev. Lett.* **72**, 1016 (1994).
- [14] R. Kraichnan, V. Yakhot, and S. Chen, *Phys. Rev. Lett.* **75**, 240 (1995).
- [15] B. I. Shraiman and E. D. Siggia, *C.R. Acad. Sci. Paris, t.321 Serie II b*, p. 279-284, (1995)
- [16] B. I. Shraiman and E. D. Siggia “Fluctuations and Mixing of a Passive Scalar in a Turbulent Flow,” preprint (1996).